

## Variational calculation of excited-state properties of a $^3\text{He}$ impurity in superfluid $^4\text{He}$

D. E. Galli, G. L. Masserini, and L. Reatto

*Istituto Nazionale di Fisica della Materia, Dipartimento di Fisica, Università di Milano, Via Celoria 16, 20133 Milano, Italy*

(Received 15 December 1998)

We report a variational Monte Carlo calculation with shadow wave function of the excited-state properties at  $T=0$  K for a system composed by one  $^3\text{He}$  atom in superfluid  $^4\text{He}$ . Explicit nonperturbative backflow contributions are used both for the collective  $^4\text{He}$  excitation and for the impurity  $^3\text{He}$  excitation. The impurity and the collective excitation states have been orthogonalized and diagonalization of the Hamiltonian has been obtained directly through the Monte Carlo calculation. This process has strong effect on some of the expectation values for the observables of the system. Energy, effective mass, and strength of the single excitation peak of the impurity are computed. Above  $q \approx 0.5 \text{ \AA}^{-1}$  the effective mass increases significantly with  $q$  but this increase is not as large as deduced from experiment. The strength of the single excitation peak in the dynamical structure factor for the  $^3\text{He}$  impurity atom is strongly reduced by an interference contribution due to  $^4\text{He}$  atoms and the resulting strength is now in good agreement with experiment. The importance of the coupling between  $^3\text{He}$  and  $^4\text{He}$  suggests the need for a reanalysis of the experimental data.

[S0163-1829(99)00829-2]

### I. INTRODUCTION

The finite solubility of  $^3\text{He}$  in  $^4\text{He}$  even at  $T=0$  K offers the possibility of studying a mixture of bosons and fermions. The situation is simpler at very low concentration of  $^3\text{He}$  when the statistical effect of the fermion component is negligible and one can consider one single impurity in a sea of  $^4\text{He}$  atoms. This system has been widely studied and it represents a severe test of many-body theory due to the presence of strong interaction effects. For instance, the excitation spectrum of the system has, in addition to the usual phonon-maxon-rotor spectrum of pure  $^4\text{He}$ , a second branch which is free-particle like,  $E(q) = \hbar^2 q^2 / 2m^*$ , at least at small wave vector.<sup>1</sup> This impurity branch, the so-called Landau-Pomeranchuk branch, has an effective mass  $m^*$  which strongly deviates from the bare mass and it is density dependent. These are typical effects of strong interaction. The accurate computation of  $m^*$  from the microscopic theory turned out to be a very difficult job.<sup>2</sup> A key effect is backflow, i.e., correlated motion of the  $^3\text{He}$  atom with the  $^4\text{He}$  ones, and this has to be treated by advanced theories in order to get reliable results.<sup>3,4</sup>

Recently the direct measurement of the excitation spectrum of a diluted solution of  $^3\text{He}$  in  $^4\text{He}$  has been performed at microscopic wave vectors by inelastic neutron scattering.<sup>5</sup> This offers the opportunity for a more detailed comparison between theory and experiment. Here we address the problem of one  $^3\text{He}$  atom in liquid  $^4\text{He}$  by the variational theory based on shadow wave function (SWF).<sup>6</sup> This technique has been found to be very useful for the study of pure liquid  $^4\text{He}$ , in particular for the study of large wave vector excitations like the rotons.<sup>7,8</sup> This approach is presently the most accurate one giving a truly quantitative description of rotons in superfluid  $^4\text{He}$  by a microscopic variational theory. A key element for this success of SWF is believed to be due to the possibility of an accurate treatment of backflow at short distance. This suggests that this technique should be useful also for the impurity problem. The result of a preliminary com-

putation has been already presented some time ago.<sup>9</sup> We have now completed this study and we have introduced a number of improvements over the earlier computation. First, as the ground state we have used fully optimized correlating factors for pure  $^4\text{He}$ , which is producing the best energy from variational Monte Carlo calculations (VMC) over the full density range.<sup>10</sup> In the second place, and most important, by using an explicit backflow term in the wave function we are able to optimize the form and intensity of backflow. Finally, we take into account that the excitation of quasiparticle character is not orthogonal to the collective excitation and a proper orthogonalization is performed by the Monte Carlo method. This is a further development of VMC. Section II contains the description of the theory and of the simulation method that we have used. The results are presented in Secs. III and Sec. IV contains the conclusion. Some details of the simulation method are presented in the Appendix.

### II. VARIATIONAL CALCULATION

#### A. The shadow wave function technique

##### 1. Ground state

For a system composed of  $N$   $^4\text{He}$  atoms and one  $^3\text{He}$  impurity we write the shadow wave function for the ground state in the form

$$\Psi_0(R) = \int dS F(R, S), \quad (1)$$

where  $R = \{\vec{r}_{\text{imp}}, \vec{r}_1, \dots, \vec{r}_N\}$  are the coordinates of the particles (the subscript imp refers to the  $^3\text{He}$  impurity variables),  $S = \{\vec{s}_{\text{imp}}, \vec{s}_1, \dots, \vec{s}_N\}$  is a set of auxiliary (shadow) variables that are integrated over the whole space. Interparticle correlations between  $^4\text{He}$  atoms and between the  $^3\text{He}$  impurity and  $^4\text{He}$  atoms are contained in

$$F(R, S) = \phi_p(R) f_{ps}^{\text{imp}}(|\vec{r}_{\text{imp}} - \vec{s}_{\text{imp}}|) \times \prod_{i=1}^N f_{ps}(|\vec{r}_i - \vec{s}_i|) \phi_s(S). \quad (2)$$

$\phi_p(R) = \prod_{i=1}^N f_p^{\text{imp}}(|\vec{r}_i - \vec{r}_{\text{imp}}|) \times \prod_{i<j=1}^N f_p(|\vec{r}_i - \vec{r}_j|)$  is a Jastrow factor, and similarly for  $\phi_s(S) = \prod_{i=1}^N f_s^{\text{imp}}(|\vec{s}_i - \vec{s}_{\text{imp}}|) \times \prod_{i<j=1}^N f_s(|\vec{s}_i - \vec{s}_j|)$ . Integration over shadow coordinates implicitly introduces correlations between particles beyond the pair (Jastrow) level at all orders. The Hamiltonian of this system is given by

$$\hat{H} = -\frac{\hbar^2}{2m_4} \sum_{i=1}^N \nabla_i^2 - \frac{\hbar^2}{2m_3} \nabla_{\text{imp}}^2 + \sum_{i<j=1}^N v(|\vec{r}_i - \vec{r}_j|) + \sum_{j=1}^N v(|\vec{r}_{\text{imp}} - \vec{r}_j|), \quad (3)$$

$m_4$  being the  $^4\text{He}$  mass. The interatomic interaction  $v(r)$  between the  $^3\text{He}$  impurity and the  $^4\text{He}$  atoms is equal to the one between  $^4\text{He}$  atoms. Therefore, the  $^3\text{He}$  atom differs from the  $^4\text{He}$  atoms only for its bare mass. For simplicity for most of the computations we have used the same correlating factors for  $^3\text{He}$ - $^4\text{He}$  as for  $^4\text{He}$ - $^4\text{He}$ . This assumption has been frequently used in the variational theory of this system. We have verified that the energy spectrum is only slightly modified when the impurity pseudopotentials weakly differ from those of bulk  $^4\text{He}$ . Here we have used the recently fully optimized<sup>10</sup> correlating factors  $f_p$ ,  $f_s$ , and  $f_{ps}$  which give the best variational Monte Carlo description of the pure  $^4\text{He}$  ground state over the full density range of the fluid phase. The accuracy of the assumption of equal  $^3\text{He}$ - $^4\text{He}$  and  $^4\text{He}$ - $^4\text{He}$  correlation has been tested computing the chemical potential of the  $^3\text{He}$  impurity. In this case  $\mu_3$  turns out to be  $\mu_3(\rho_{\text{eq}}) = -2.43 \pm 0.01$  K with an experimental data of  $\mu_3(\rho_{\text{eq}}) = -2.78$  K,<sup>11</sup> and  $\mu_3(1.16\rho_{\text{eq}}) = 5.29 \pm 0.03$  K in agreement with the increase of the experimental value ( $\mu_3 \sim 5$  K at  $\rho \approx 1.16\rho_{\text{eq}}$ ). The excitation energies are obtained as difference between the total energy of the excited state and the total ground-state energy; a good choice of the ground-state wave function is, therefore, important in order to guarantee that the excitation energies are not affected by a poor variational ground state.

## 2. Excited states

It is known that shadow variables are a way to represent in  $\Psi_0(R)$  the correlation effects of quantum delocalization of hard-core particles. The representation of excited states with a shadow wave function is based on the hypothesis that the correlations effects of quantum delocalization of hard-core particles should be present also in the excited-states of low energy. This suggested<sup>12</sup> to extend to shadow variables the Feynman ansatz<sup>13</sup> for the excited state wave function, i.e., the phase factors of the excited states were written in terms of the shadow variables. It is known<sup>14</sup> that introducing the phase in the subsidiary variables is a way to incorporate implicitly backflow up to high order in the real variables. This already accounts for most of the effects of backflow but in order to obtain really accurate results for the roton energy it is necessary to introduce an explicit backflow contribution

in the wave function.<sup>15</sup> We extend this approach to the case of the impurity and we write the shadow wave function for an excited  $^3\text{He}$  atom in the form

$$\Psi_q^I(R) = \int dS F(R, S) \tilde{\delta}_q^I, \quad (4)$$

whereas the wave function for the collective excited state of the  $N$   $^4\text{He}$  atoms is taken to be

$$\Psi_q^B(R) = \int dS F(R, S) \tilde{\sigma}_q^B. \quad (5)$$

The momentum carrying factors read

$$\tilde{\delta}_q^I = e^{i\vec{q} \cdot \vec{s}_{\text{imp}}}, \quad \tilde{\sigma}_q^B = \sum_{j=1}^N e^{i\vec{q} \cdot \vec{s}_j}. \quad (6)$$

They are expressed in terms of the shadow variables:  $\vec{s}$  represents a shadow variable modified by an explicit backflow term

$$\vec{s}_j = \vec{s}_j + \sum_{l(\neq j)} (\vec{s}_j - \vec{s}_l) \lambda(s_{jl}), \quad (7)$$

and a similar expression is assumed for  $\vec{s}_{\text{imp}}$ . For  $\lambda(s)$  we have assumed the same short-range form,  $\lambda(s) = \alpha(s/r_0 - 2)^2 \exp\{-[(s-r_0/w)]^2\}$  for  $s < 2r_0$ ,  $\lambda(s) = 0$  for  $s > 2r_0$ , already used in the calculation of the excitation spectrum in the pure  $^4\text{He}$  system. As already noticed even when the amplitude of the explicit backflow is zero these wave functions contain backflow effects in an implicit way. In fact in a previous computation with  $\alpha = 0$  we found<sup>9</sup> that the effective mass of the impurity given by Eq. (4) differs from the bare mass of  $^3\text{He}$ . We find that the presence of the explicit backflow contributions in  $\tilde{\sigma}_q^B$  and in  $\tilde{\delta}_q^I$  lowers the energy and in this way we obtain the variational determination of the range and of the amplitude of the backflow via the parameters  $\alpha$ ,  $r_0$ , and  $w$ . Notice that the explicit backflow is in the exponential form and no expansion is performed. In principle, the variational backflow parameters  $\alpha$ ,  $r_0$ , and  $w$  are wave-vector dependent and the optimal ones for the excited state  $\Psi_q^I$  could be different from those optimal for the excited state  $\Psi_q^B$ . Our strategy has been to use for the excited state  $\Psi_q^B$  the variational backflow parameters  $\alpha$ ,  $r_0$ , and  $w$  which have been optimized in an excitation spectrum calculation in pure  $^4\text{He}$ . This is not a true limitation because we expect that the presence of one  $^3\text{He}$  atom in the system does not change appreciably the optimal backflow to be used in  $\Psi_q^B$ . The optimal variational backflow parameters in  $\Psi_q^I$  have been obtained performing a preliminary computation of the ‘‘excitation energy’’

$$E^I(q) = \frac{\langle \Psi_q^I | \hat{H} | \Psi_q^I \rangle}{\langle \Psi_q^I | \Psi_q^I \rangle} - \frac{\langle \Psi_0 | \hat{H} | \Psi_0 \rangle}{\langle \Psi_0 | \Psi_0 \rangle}. \quad (8)$$

We find that the optimal backflow parameters of the impurity in superfluid  $^4\text{He}$ , are essentially independent of  $q$  and they coincide with those of the roton excitation in pure  $^4\text{He}$  ( $r_0 = 2.81$  Å and  $\alpha = 0.3$  at both densities,  $w = 1.53$  Å at equi-

librium density and  $w = 1.02 \text{ \AA}$  at freezing density). These values are similar to what we found previously<sup>7,8</sup> for the excitation spectrum of one distinguishable  $^4\text{He}$  atom.

The shadow wave functions (4) and (5) are eigenstates of momentum  $\vec{p} = \hbar\vec{q}$ , so Eqs. (4) and (5) are orthogonal to the ground state (1) (and of course also to the true ground state) but they are not orthogonal between each other. Therefore, these wave functions do not give a proper treatment of the two branches of excitations. We have corrected this situation explicitly by building proper orthonormal excited states and by performing the Hamiltonian diagonalization directly through a Monte Carlo calculation as explained in the next subsection.

### B. Orthogonalization process and Hamiltonian diagonalization

Starting from the wave functions  $\Psi_q^I$  and  $\Psi_q^B$  let us consider the normalized functions

$$\bar{\Psi}_q^I = \frac{\Psi_q^I}{\sqrt{\langle \Psi_q^I | \Psi_q^I \rangle}}, \quad \bar{\Psi}_q^B = \frac{\Psi_q^B}{\sqrt{\langle \Psi_q^B | \Psi_q^B \rangle}}. \quad (9)$$

Second, we fix one excited state to be represented by the wave function  $\bar{\Psi}_q^B$  and obtain the other orthonormal excited state  $\bar{\Psi}_q^{I'}$  as linear complex combination of the states (9)

$$\bar{\Psi}_q^{I'} = \frac{\bar{\Psi}_q^I - \langle \bar{\Psi}_q^B | \bar{\Psi}_q^I \rangle \bar{\Psi}_q^B}{\sqrt{1 - |\langle \bar{\Psi}_q^B | \bar{\Psi}_q^I \rangle|^2}}, \quad (10)$$

such that  $\langle \bar{\Psi}_q^{I'} | \bar{\Psi}_q^B \rangle = 0$  and  $\langle \bar{\Psi}_q^{I'} | \bar{\Psi}_q^{I'} \rangle = 1$ . This is no more than a Gram-Schmidt orthonormalization method applied to Eqs. (4) and (5). Now we have the two orthonormal states  $\bar{\Psi}_q^{I'}$  and  $\bar{\Psi}_q^B$  which are again orthogonal to the ground state and eigenstates of momentum  $\vec{p} = \hbar\vec{q}$ . The Hamiltonian (3) is not diagonal in this basis; i.e., the  $2 \times 2$  matrix

$$\mathbf{H} = \begin{pmatrix} \langle \bar{\Psi}_q^{I'} | \hat{H} | \bar{\Psi}_q^{I'} \rangle & \langle \bar{\Psi}_q^{I'} | \hat{H} | \bar{\Psi}_q^B \rangle \\ \langle \bar{\Psi}_q^B | \hat{H} | \bar{\Psi}_q^{I'} \rangle & \langle \bar{\Psi}_q^B | \hat{H} | \bar{\Psi}_q^B \rangle \end{pmatrix} = \begin{pmatrix} H_{11} & H_{12} \\ H_{21} & H_{22} \end{pmatrix} \quad (11)$$

has the off-diagonal complex elements  $H_{12}$  and  $H_{21} (= H_{12}^*)$  different from zero. We must search for the unitary transformation  $\mathbf{U}$  ( $\mathbf{U}\mathbf{U}^\dagger = \mathbf{1}$ ) which gives

$$\mathbf{U}\mathbf{H}\mathbf{U}^\dagger = \begin{pmatrix} \lambda_1 & 0 \\ 0 & \lambda_2 \end{pmatrix}, \quad (12)$$

where  $\lambda_1$  and  $\lambda_2$  are the eigenvalues of  $\mathbf{H}$

$$\lambda_{1,2} = \frac{1}{2} [H_{11} + H_{22} \pm \sqrt{(H_{11} - H_{22})^2 + 4|H_{12}|^2}] \quad (13)$$

(note that even if not expressed  $\lambda_1$ ,  $\lambda_2$ , and  $H_{ij}$  are wave-vector  $q$  dependent). The corresponding wave functions which give the diagonal representation of the Hamiltonian read

$$\Psi_q^{(1)} = \zeta[\bar{\Psi}_q^{I'} + \theta^* \bar{\Psi}_q^B], \quad \Psi_q^{(2)} = \zeta[\theta \bar{\Psi}_q^{I'} - \bar{\Psi}_q^B], \quad (14)$$

where

$$\zeta = \sqrt{\frac{H_{11} - H_{22} + \gamma}{2\gamma}}, \quad \theta = \frac{2H_{12}}{H_{11} - H_{22} + \gamma}, \quad (15)$$

$$\gamma = \sqrt{(H_{11} - H_{22})^2 + 4|H_{12}|^2}.$$

The excited states (14) are clearly derived only formally and they cannot be used directly in a Monte Carlo integration. We do not need to do this however, because the expectation value of an observable  $\hat{O}$  with respect to  $\bar{\Psi}_q^{(1)}$ , and  $\bar{\Psi}_q^{(2)}$  can be expressed in terms of  $\langle \bar{\Psi}_q^I | \hat{O} | \bar{\Psi}_q^I \rangle$ ,  $\langle \bar{\Psi}_q^B | \hat{O} | \bar{\Psi}_q^B \rangle$ ,  $\langle \bar{\Psi}_q^I | \hat{O} | \bar{\Psi}_q^B \rangle$ , and  $\langle \bar{\Psi}_q^I | \bar{\Psi}_q^B \rangle$  as derivable from Eqs. (14) and (10). These matrix elements can be computed directly during the Monte Carlo calculation using a reweighting technique to avoid the sign problem; this technique is described in detail in the Appendix. The Hamiltonian diagonalization is therefore obtained as algebraic combinations of this set of basic integrals evaluated by Monte Carlo integration.

## III. RESULTS

### A. Energy spectrum

As interatomic interaction we have used the Aziz<sup>16</sup> potential. In Fig. 1 we display the two branches of the excitation spectrum computed in a system with one  $^3\text{He}$  impurity and 107  $^4\text{He}$  atoms over the full momentum range at the equilibrium density  $\rho_{\text{eq}} = 0.0218 \text{ \AA}^{-3}$  and at  $1.2\rho_{\text{eq}}$ . Our computation can be performed only for a discrete set of  $q$  values such that the periodic boundary conditions are satisfied. Experimental data for the energy spectrum are available only for wave vectors  $q \approx 1.7 \text{ \AA}^{-1}$  at  $\rho_{\text{eq}}$  and at  $\rho = 1.15\rho_{\text{eq}}$ . Beyond this wave vector the peak in the dynamic structure factor,  $S(q, \omega)$ , due to the quasiparticle  $^3\text{He}$  excitation overlaps the one of the collective  $^4\text{He}$  excitation of the system. For the wave vector beyond the crossing the quasiparticle  $^3\text{He}$  excitation has not been observed and it is not a stable excitation because it can decay into the collective  $^4\text{He}$  excitation. In our theory no lifetime effect is present and we obtain a well-defined excitation energy also at large momenta. The theoretical quasiparticle excitation spectrum shows deviations from a simple parabola, but it can be represented by  $E(q) = \hbar^2 q^2 / 2m^*(q)$ , where the effective mass  $m^*(q)$  is a function of  $q$  and it increases significantly with  $q$ . The values for the effective mass range from  $2.09m_3$  to  $2.26m_3$  between  $q = 0.37$  and  $1.7 \text{ \AA}^{-1}$  at  $\rho_{\text{eq}}$ , and from  $2.71m_3$  to  $2.93m_3$  between  $q = 0.39$  and  $1.8 \text{ \AA}^{-1}$  at  $1.2\rho_{\text{eq}}$ . There is no roton minimum in the dispersion relation neither at  $\rho_{\text{eq}}$  nor at  $1.2\rho_{\text{eq}}$ . The orthogonalization-diagonalization process has little effect on the  $^3\text{He}$  quasiparticle excitation branch which, after this process, remains substantially equal to the excitation energy computed through Eq. (8). The situation is completely different for the collective  $^4\text{He}$  excitation which underestimates the excitation energies in the maxon and high-phonon regions of the spectrum if the orthogonalization-diagonalization process is not introduced (see Fig. 2). Our results for the energy of the quasiparticle branch are in good agreement with the neutron-scattering results at the lowest measured  $q$ , around  $1 \text{ \AA}^{-1}$ . At larger  $q$  there is an increas-

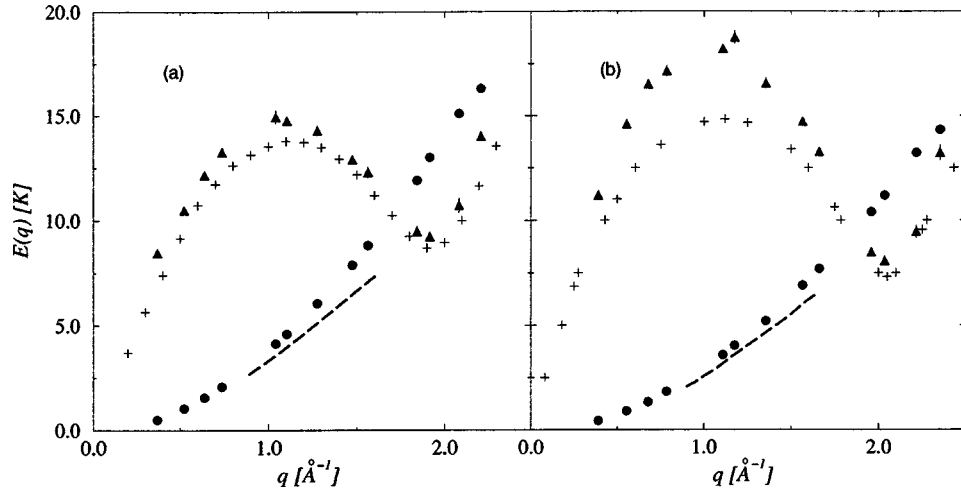


FIG. 1. (a) Excitation spectrum at  $\rho_{\text{eq}}$ ; (circles)  ${}^3\text{He}$  quasiparticle excitation branch, (triangles) collective  ${}^4\text{He}$  excitation branch, (plus) experimental excitation spectrum in pure  ${}^4\text{He}$ , (dashed line) experimental  ${}^3\text{He}$  quasiparticle excitation branch. (b) the same as (a) at  $1.2\rho_{\text{eq}}$ ; here the experimental  ${}^3\text{He}$  quasiparticle excitation branch is measured at 18 bars ( $\rho \approx 1.15\rho_{\text{eq}}$ ). When not reported, error bars are less than the symbol size.

ing deviation between our results and experiment, the experimental  $\epsilon(q)$  having much less curvature. Similar behavior is found at higher density.

Our computed impurity spectrum can be represented quite accurately by a simple analytical expression, either by  $E(q) = \hbar^2 q^2 (1 + aq^2) / 2m^*$  or by  $E(q) = \hbar^2 q^2 / [2m^* (1 + bq^2)]$  with  $m^*$ ,  $a$ , and  $b$  as fitted parameters (see Fig. 3). These forms have been already used by Fåk *et al.*<sup>5</sup> to fit their experimental data. We find that these expressions give a good representation of our result for  $E_q$  over the full  $q$  range of our computation. From the fit of our data with these two formulas we find similar values of the effective mass  $m^*$  at  $q=0$  for the  ${}^3\text{He}$  impurity; we obtain the values  $m^* = (2.075 \pm 0.013)m_3$  with  $a = -0.0269 \pm 0.0019 \text{ \AA}^2$  and  $m^* = (2.065 \pm 0.014)m_3$  with  $b = 0.0314 \pm 0.0022 \text{ \AA}^2$  at  $\rho_{\text{eq}}$ ;  $m^* = (2.714 \pm 0.014)m_3$  with  $a = -0.0213$

$\pm 0.0016 \text{ \AA}^2$  and  $m^* = (2.708 \pm 0.015)m_3$  with  $b = 0.0241 \pm 0.0019 \text{ \AA}^2$  at  $1.2\rho_{\text{eq}}$ . Our result agrees very well with the recent accurate measurement<sup>17,18</sup> by Yorozu *et al.*, as well as by Simons and Mueller, when the experimental data for the effective mass (at  $q=0$ )  $m^*$  are extrapolated to zero concentration taking into account the Fermi-liquid effects as suggested<sup>19,4</sup> by Krotschek *et al.*:  $m^* \approx 2.16m_3$  at  $\rho_{\text{eq}}$  and considering the results for positive pressure one can extrapolate the value  $m^* \approx 2.74m_3$  at freezing ( $1.2\rho_{\text{eq}}$ ). Our system in fact is at finite concentration of  ${}^3\text{He}$  but it has no Fermi statistic effects because of the presence of one single  ${}^3\text{He}$  atom in the simulation box.

The orthogonalization-diagonalization process has a small effect on the quasiparticle spectrum and therefore on the extrapolated value for the effective mass  $m^*$ . Without this process the effective mass  $m^*$  at  $q=0$  for the  ${}^3\text{He}$  impurity turns out to be  $m^* = (2.049 \pm 0.012)m_3$  with  $a = -0.0308 \pm 0.0018 \text{ \AA}^2$  and  $m^* = (2.036 \pm 0.014)m_3$  with  $b = 0.0369 \pm 0.0022 \text{ \AA}^2$ . Because the orthogonalization-diagonalization process has a small effect on the quasiparticle spectrum, one can see the importance of the inclusion in the SWF (4) of the explicit backflow term by comparing in Fig. 2 our previous result<sup>9</sup> for the quasiparticle spectrum with the new one. In that calculation the backflow was not optimized because no explicit backflow terms were introduced; the effective mass extrapolated at  $\rho_{\text{eq}}$  at  $q=0$  was only  $m^* = 1.74m_3$ . A strong discrepancy is instead present in the coefficients  $a$  or  $b$  giving the  $q$  dependence of  $m^*(q)$ , the theoretical value being about four times smaller than the experimental value<sup>5</sup> at equilibrium density and about three times smaller at the larger density. This could be a genuine discrepancy due to a defect of the theory, either the assumed form of our excitation operator (4), (5) or the assumption that the ground-state correlating factors do not distinguish between  ${}^3\text{He}$  and  ${}^4\text{He}$ . However, it should be kept in mind that the analysis of the scattering data<sup>5</sup> has been performed with a number of approximations and these could affect the extracted energy spectrum. The experiment is performed at a finite concentration so that the  ${}^3\text{He}$  signal consists of a particle-hole band

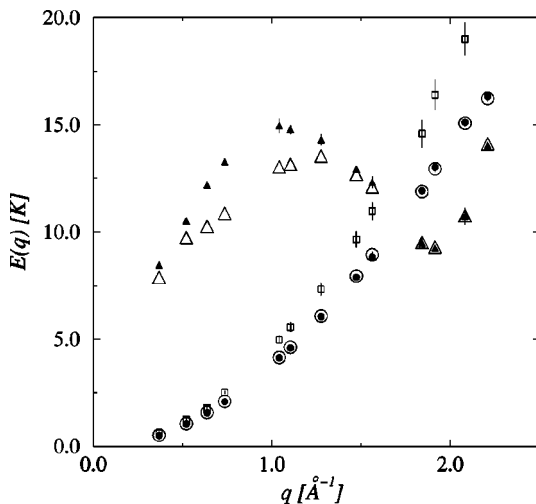


FIG. 2. Excitation spectrum at  $\rho_{\text{eq}}$  as in Fig. 1; open and full circles and triangles represent, respectively, the computed two branches of the spectrum before and after the orthogonalization-diagonalization process. Squares represent the quasiparticle excitation spectrum at  $\rho_{\text{eq}}$  computed without the explicit backflow term and without the orthogonalization-diagonalization process (Ref. 9).

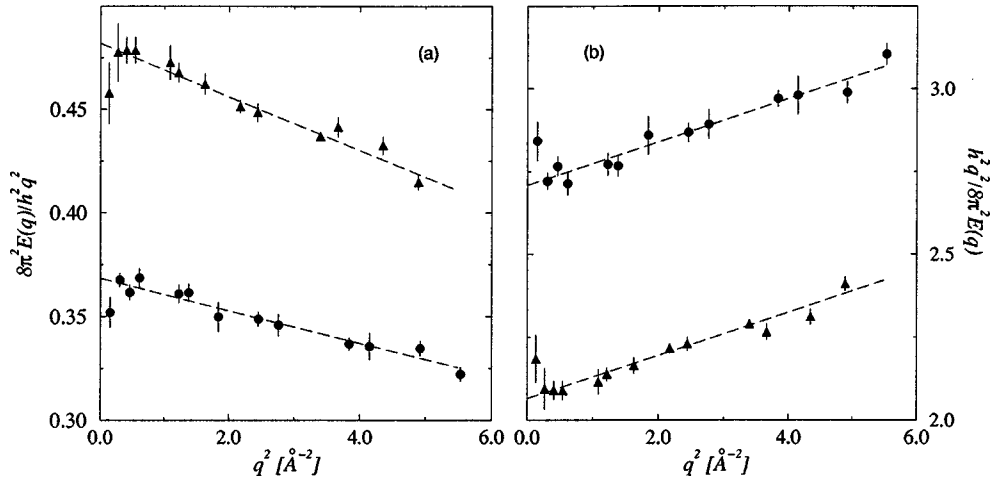


FIG. 3. (a)  $2E(q)/\hbar^2 q^2$  as function of  $q^2$  at  $\rho_{\text{eq}}$  (triangles) and at  $1.2\rho_{\text{eq}}$  (circles). The linear fit is also reported; the intercept gives the value of  $1/m^*$ . (b)  $\hbar^2 q^2 / 2E(q)$  for the same data in (a). Here the intercept gives the value of  $m^*$ .

due to Fermi statistics. It has been assumed that the maximum of the observed band coincides with the quasiparticle energy  $E(q)$ . This is correct, for  $q$  larger than the Fermi wave vector  $k_F$ , in the case of independent particles with a quadratic spectrum in  $q$ . Both of these features are not correct in the present case, a strong interacting system. In addition, another assumption could modify the extracted energy spectrum: the neglect in the scattering cross section of the interference contribution between  $^3\text{He}$  and  $^4\text{He}$  atoms. As discussed in the next subsection we find that under the condition of the experiment the interference contribution to the quasiparticle peak is similar in magnitude to the  $^3\text{He}$  contribution and it has the opposite sign. This is similar to what Krotscheck and Saarela<sup>20</sup> found from a computation of this interference contribution at a finite concentration (5%) of  $^3\text{He}$  using the correlated basis function (CBF) technique based on a very simplified theory, the random-phase approximation. They found that the assumption that the interference contribution is negligible compared to the direct contribution is not justified; moreover they also computed the  $\omega$  dependence of this interference contribution which at large  $q$  turns out to be skewed with respect to the direct contribution thus inducing a displacement of the overall peak. A possible origin of this skewedness is the strong  $q$  dependence of the backflow of  $^4\text{He}$ .

We compare now our results with other theories. The main approach which has been used is the correlated basis function at various levels of approximation, and almost always only the effective mass at  $q=0$  has been computed. Going beyond second-order perturbation theory<sup>2</sup> with a one-phonon intermediate state gives an incomplete correction to the bare mass,  $m^* \sim 1.8m_3$ . By using two independent phonon states  $m^*$  increases to  $2.1m_3$  at equilibrium density and only by including an infinite number of rescattering processes of the one-phonon states one finds a value  $m^* = 2.2m_3$ . This is close to what we find. Recently<sup>3</sup> this scheme of computation has been extended at finite- $q$  vectors and the authors find an increasing value of the effective mass with  $q$ , in good agreement with experiment. Unfortunately such a CBF computation needs the triplet correlation function  $g_3(\vec{r}_1, \vec{r}_2, \vec{r}_3)$  which is not known and some approximation has to be introduced. The results at large  $q$  depend rather

heavily on the approximation used for  $g_3$ , either the convolution or the Kirkwood approximation, and a further element of empirical character is the use of the experimental excitation spectrum of bulk helium in the energy denominators. Similar approximations are present in the recent work<sup>4</sup> of Krotscheck *et al.* where CBF theory to infinite order and the equations of motions method have been used to compute the effective mass also at higher density. Our computation is that of  $E(q)$  at finite  $q$  in which backflow is treated at high order without introducing uncontrolled approximations.

Once the orthogonalization-diagonalization process has been performed, we find that the presence of the  $^3\text{He}$  impurity in the system has very little effect on the collective  $^4\text{He}$  excitation branch both at equilibrium and at freezing density. Comparing these collective branches with those calculated in the pure  $^4\text{He}$  system at the same density we find no substantial differences within the statistical errors. This behavior is in agreement with experimental data of the collective  $^4\text{He}$  excitation branch where it has been found that the deviation from the excitation spectrum in the pure  $^4\text{He}$  system is always less than 0.2 K. As in the pure  $^4\text{He}$  system, at freezing density there is a significant disagreement with the experimental data for the excitation spectrum in the maxon region. Here the experimental spectrum is about twice the roton energy at the same density, so that we should expect that these excitations are a mixture of single excitations and double roton excitations. The relevance of this argument was proved<sup>7</sup> by computing the excitation energy of double roton excited states in the pure  $^4\text{He}$  system and finding that in the maxon region at freezing density the energy of a double excitation is below the one of the single excitation and close to experiment.

### B. Scattering strength

In addition to energy an important quantity is the strength of the quasiparticle peak in the scattering cross section. This quantity, in fact, is sensitive to details of the wave function of the excited state. In the case of bulk  $^4\text{He}$  the analogous strength of the roton peak has been a severe test for the theory. We present now a quantitative microscopic compu-

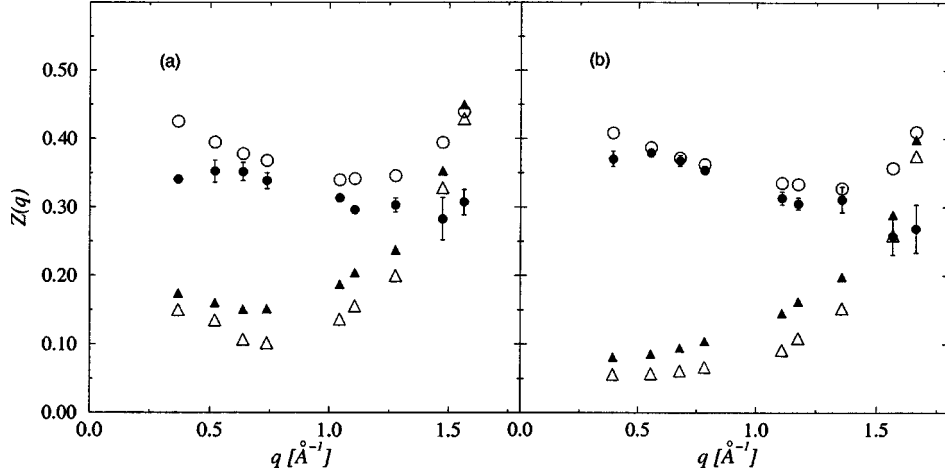


FIG. 4. (a) (full circles) results at  $\rho_{\text{eq}}$  for the intensity of the excitation peak in  $S(\vec{q}, \omega)$  for the quasiparticle  ${}^3\text{He}$  excitation, (triangles) intensity of the excitation peak in  $S(\vec{q}, \omega)$  for the collective  ${}^4\text{He}$  excitation. The open circles represent the intensity of the excitation peak for the quasiparticle  ${}^3\text{He}$  excitation computed without the orthogonalization-diagonalization process. (b) the same as (a) at  $1.2\rho_{\text{eq}}$ .

tation of the strength  $Z(q)$  of the excitation peak in  $S(q, \omega)$  for the quasiparticle  ${}^3\text{He}$  excitation which includes the contribution coming from the  ${}^4\text{He}$  atoms. In a neutron-inelastic-scattering experiment the measured quantity is the double-differential cross section. In our system, with only one  ${}^3\text{He}$  impurity, the density spin fluctuations are not present, so the double-differential cross section is given by the expression<sup>5</sup>

$$\frac{d^2\sigma}{d\Omega dE_1} = \frac{k_1}{k_0} \frac{1}{4\pi\hbar} \{ \sigma_4 x_4 S_{44}(\vec{q}, \omega) + (\sigma_3 + \sigma_3^i) x_3 S_{33}(\vec{q}, \omega) + \sigma_{34} [x_3 x_4]^{1/2} S_{34}(\vec{q}, \omega) \}, \quad (16)$$

where the dynamical structure factor  $S_{ij}(\vec{q}, \omega)$  at  $T=0$  K is given by

$$S_{ij}(\vec{q}, \omega) = \frac{1}{2\sqrt{N_i N_j}} \sum_n [\langle 0 | \rho_{-q}^i | n \rangle \langle n | \rho_q^j | 0 \rangle + \langle 0 | \rho_{-q}^j | n \rangle \langle n | \rho_q^i | 0 \rangle] \delta(\omega - \omega_n). \quad (17)$$

$\rho_q^{i(j)}$  are the density fluctuation of the  $i(j)$  component of the mixture and  $\{|n\rangle\}$  ( $n=0,1,2,\dots$ ) is an orthonormal complete set of eigenstates of the Hamiltonian with energies  $\hbar\omega_n$ .  $\sigma_4$ ,  $\sigma_3$ ,  $\sigma_3^i$ ,  $\sigma_{34}$  are the scattering cross sections,<sup>21</sup>  $x_3 = N_3/(N_3 + N_4)$  and  $x_4 = N_4/(N_3 + N_4)$  are the concentration of the  ${}^3\text{He}$  impurity and of the  ${}^4\text{He}$  atoms in the system<sup>23</sup> ( $x_3 = 1/108$  and  $x_4 = 107/108$  in our case). The amplitudes of the excitation peaks in  $S_{ij}$  are therefore given by

$$Z_{ij}^{(l)}(q) = \frac{1}{2\sqrt{N_i N_j}} \left[ \frac{\langle \Psi_0 | \rho_{-q}^i | \bar{\Psi}_q^{(l)} \rangle \langle \bar{\Psi}_q^{(l)} | \rho_q^j | \Psi_0 \rangle}{\langle \Psi_0 | \Psi_0 \rangle} + \frac{\langle \Psi_0 | \rho_{-q}^j | \bar{\Psi}_q^{(l)} \rangle \langle \bar{\Psi}_q^{(l)} | \rho_q^i | \Psi_0 \rangle}{\langle \Psi_0 | \Psi_0 \rangle} \right], \quad (18)$$

where  $\bar{\Psi}_q^{(l)}$  can be either  $\bar{\Psi}_q^{(1)}$  or  $\bar{\Psi}_q^{(2)}$  and  $\Psi_0$  is the ground state (1). The expectation values in Eq. (18) cannot be computed directly. Like in the case of the Hamiltonian diagonalization, one must write Eq. (18) as an algebraic combination

of a set of matrix elements built with the wave functions  $\Psi_0$ ,  $\Psi_q^I$ , and  $\Psi_q^B$ , as derivable from Eq. (14); these quantities are all computable by a reweighting technique via direct Monte Carlo integration as shown in the Appendix.

In order to obtain the correct comparison between the experimental data<sup>5</sup> and our results, we have defined the intensity  $Z^{\text{imp}}(q)$  of the excitation peak for the  ${}^3\text{He}$  impurity branch normalizing the total scattering contribution with the factor  $x_3(\sigma_3 + \sigma_3^i)$  as done in Ref. 5:

$$Z^{\text{imp}}(q) = Z_{33}^{\text{imp}}(q) + \frac{\sigma_4}{\sigma_3 + \sigma_3^i} \frac{x_4}{x_3} Z_{44}^{\text{imp}}(q) + \frac{\sigma_{34}}{\sigma_3 + \sigma_3^i} \sqrt{\frac{x_4}{x_3}} Z_{34}^{\text{imp}}(q) = Z_{33}^{\text{imp}}(q) + c_1 Z_{44}^{\text{imp}}(q) + c_2 Z_{34}^{\text{imp}}(q), \quad (19)$$

where the last equality defines  $c_1$  and  $c_2$ . The superscript imp means that of the two excited-state wave functions  $\bar{\Psi}^{(l)}$  in Eq. (14) the one has been used which corresponds to the quasiparticle  ${}^3\text{He}$  excitation. In Fig. 4 we report our results for the intensity of the peak for the impurity excitation at  $\rho_{\text{eq}}$  and  $1.2\rho_{\text{eq}}$  for wave vectors up to the crossing region with the collective excitation.

The quasiparticle  ${}^3\text{He}$  excitation is decoupled from the variables of  ${}^4\text{He}$  atoms when no backflow is present; in this case  $Z_{34}^{\text{imp}}(q) = Z_{44}^{\text{imp}}(q) = 0$  and  $Z_{33}^{\text{imp}}(q) = 1 \forall q$ . Experimentally has been found a much smaller value for  $Z^{\text{imp}}$ , of order of 1/3 and no explanation was given. On the basis of sum rule arguments it has been suggested<sup>22</sup> that the depression of  $Z^{\text{imp}}$  could be due to the interference contribution  $Z_{34}^{\text{imp}}$  but no quantitative computation was presented. As already mentioned, Krotscheck and Saarela<sup>20</sup> computed the dynamic structure factors  $S_{33}(\vec{q}, \omega)$ ,  $S_{44}(\vec{q}, \omega)$ , and  $S_{34}(\vec{q}, \omega)$  at a finite concentration (5%) of  ${}^3\text{He}$  on the basis of a very simplified theory. They found that the particle-hole  ${}^3\text{He}$  continuum is not negligible in the  ${}^4\text{He}$ - ${}^4\text{He}$  channel, neither is the collective mode in the  ${}^3\text{He}$ - ${}^3\text{He}$  channel and also that the assumption that  $S_{34}(\vec{q}, \omega)$  is negligible compared to the di-

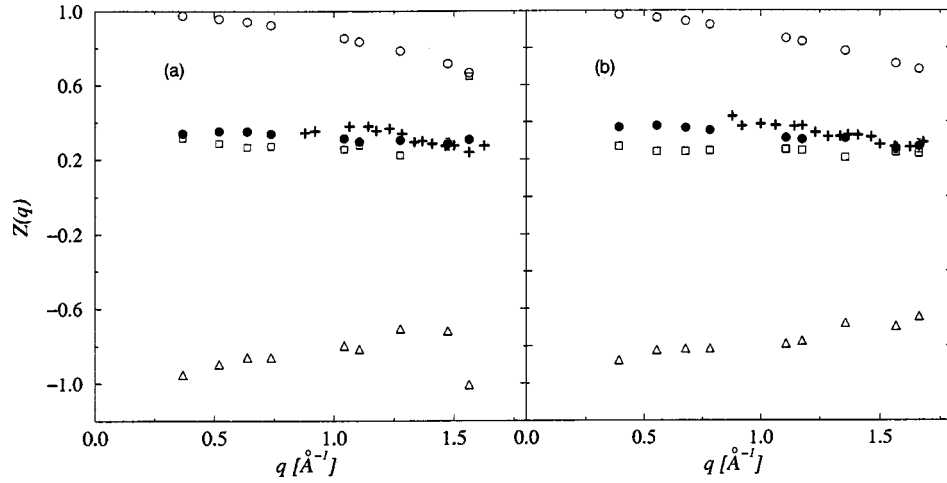


FIG. 5. (a) (full circles)  $Z^{\text{imp}}(q)$  at  $\rho_{\text{eq}}$ , (plus) experimental data for  $Z^{\text{imp}}(q)$ , (open circles)  $Z_{33}^{\text{imp}}(q)$ , (squares)  $c_1 Z_{44}^{\text{imp}}(q)$ , (triangles)  $c_2 Z_{34}^{\text{imp}}(q)$ ; (b) the same as (a) at  $1.2\rho_{\text{eq}}$ .

agonal terms is not justified. Our results agree with these previous qualitative results and we are able now to give a quantitative description of these effects. We indeed find that both contributions  $Z_{34}^{\text{imp}}(q)$  and  $Z_{44}^{\text{imp}}(q)$  are quite important at all wave vectors and the results are shown in Fig. 5. It can be noticed that  $c_2 Z_{34}^{\text{imp}}(q)$  is negative and almost as large as  $Z_{33}^{\text{imp}}(q)$  so that there is a very large cancellation and the weaker  $c_1 Z_{44}^{\text{imp}}(q)$  turns out to represent a rather large part of the total  $Z^{\text{imp}}$ . This is true both at equilibrium density and at freezing. We can also notice that these strengths  $Z_{\alpha\beta}^{\text{imp}}$  depend rather strongly on the orthogonalization-diagonalization process as can be seen in Fig. 4.

The strength  $Z^{\text{imp}}$  deduced from experiment is also shown in Fig. 5. We note the excellent agreement with our results. Also the weak density dependence of  $Z^{\text{imp}}$  found experimentally agrees with our result. All this allows us to conclude that the experimental “missing” intensity in  $Z^{\text{imp}}(q)$  is due to the coupling between  ${}^3\text{He}$  and  ${}^4\text{He}$  arising from strong backflow effects. In the case of rotons in pure  ${}^4\text{He}$  backflow reduces the intensity of the roton peak in  $S(q, \omega)$  by about 30% compared with the result expected in the absence of backflow (the Feynman description of a roton). The backflow effect is even stronger in the case of the impurity excitation where the reduction is about 70%. As mentioned in the previous subsection our results suggest the need for a reanalysis of the experimental data. In fact the data has been analyzed under the assumption that only  $S_{33}(q, \omega)$  gives strength to the impurity branch. This assumption, which has been shown not to be correct by our computation, would not affect the extracted energy spectrum  $E_{\text{imp}}(q)$  if the  $\omega$  dependence of  $S_{34}(q, \omega)$  and  $S_{44}(q, \omega)$  were the same as that of  $S_{33}(q, \omega)$ . Unfortunately our theory is not able to give these  $\omega$  dependences but the result of Ref. 20 indicates that this is not the case at large  $q$  where  $S_{34}$  is asymmetric and skewed toward larger frequencies compared with  $S_{33}$ . This suggests that the analysis of the experimental data in Ref. 5 has overestimated  $E_{\text{imp}}(q)$  at large  $q$ .

Very recently<sup>4</sup> Krotscheck *et al.* computed the strength  $Z(q)$  of the excitation peak in  $S_{33}(q, \omega)$  for the quasiparticle  ${}^3\text{He}$  excitation for a system composed of one single  ${}^3\text{He}$  atom in bulk  ${}^4\text{He}$ . Their  $Z(q)$  agrees with experimental data

even if they do not consider the contribution due to  $S_{34}$  and  $S_{44}$ . This is rather surprising in view of our results and an extension of the theory of Ref. 4 to include such interference effects should be important.

#### IV. CONCLUSION

We have extended our previous computation of the excitation spectrum of one  ${}^3\text{He}$  impurity in liquid  ${}^4\text{He}$  by the shadow wave function technique by including an explicit backflow contribution and by using improved ground-state pseudopotentials. We have also introduced a methodological improvement. It is customary with the CBF method to start with nonorthogonal states which are then orthonormalized. This is not usually done in the framework of the Monte Carlo method. Here we start from trial wave functions for the single particle and for the collective excitations which are not orthogonal to each other. We have shown that the needed orthogonalization of the states and the diagonalization of the Hamiltonian are feasible within the Monte Carlo method. The present case, with just two states for each wave vector, is rather simple and it will be important to verify if this procedure is also possible in cases in which a larger set of states is involved.

The present computation confirms that with the shadow technique starting with a rather simple ansatz for the states, one is able to include backflow effects to high order. In fact we find an effective mass at small  $q$  which is similar to what is found with an infinite order calculation within the CBF formalism. Our result is in good agreement with experiment both at equilibrium and at freezing density. Less satisfactory appears to be the momentum dependence of  $m^*$  which is much smaller than what has been deduced from neutron-scattering data. Perhaps the most important aspect of our computation is the first quantitative computation of the strength of the single-particle peak in the neutron-scattering cross section which includes the strength coming not only from the  ${}^3\text{He}$  atom but also from the  ${}^4\text{He}$  atoms. These processes give strength to the impurity peak via backflow. We find that these processes give a major contribution, especially the  ${}^3\text{He}$ - ${}^4\text{He}$  interference term. With the present

theory we now find good agreement with experiment for the total strength of the impurity peak. However, our results suggest that the impurity excitation energy deduced from experiment might need a reanalysis by including in the treatment of the data the contributions coming both from the  $^3\text{He}$ - $^4\text{He}$  channel and from the  $^4\text{He}$ - $^4\text{He}$  one. This should not affect the strength of the impurity excitation branch but it might affect its energy.

#### ACKNOWLEDGMENTS

This work has been supported by INFN under Progetto di Supercalcolo. It was conducted using the CINECA supercomputer resources (CRAY-T3E).

#### APPENDIX

As a trivial exercise one can easily verify that every expectation values of the form  $\langle \Psi_q^{(i)} | \hat{O} | \Psi_q^{(j)} \rangle$  (with  $i, j = 1, 2$ ) can be written as algebraic combination of the matrix elements  $\langle \bar{\Psi}_q^L | \hat{O} | \bar{\Psi}_q^L \rangle$ ,  $\langle \bar{\Psi}_q^B | \hat{O} | \bar{\Psi}_q^B \rangle$ ,  $\langle \bar{\Psi}_q^L | \hat{O} | \bar{\Psi}_q^B \rangle$ , and  $\langle \bar{\Psi}_q^L | \Psi_q^B \rangle$  using Eqs. (14), (15), and (10). This is true also in the calculation of the contributions to the intensity of the excitation peaks in the dynamical structure factor where the matrix elements of the form  $\langle \bar{\Psi}_q^{(l)} | \rho_q^j | \Psi_0 \rangle / \langle \Psi_0 | \Psi_0 \rangle^{1/2}$  ( $l = 1, 2$  and  $j = 3, 4$ ) can be written as algebraic combination of those of the type  $\langle \bar{\Psi}_q^L | \rho_q^j | \Psi_0 \rangle / \langle \Psi_0 | \Psi_0 \rangle^{1/2}$ ,  $\langle \bar{\Psi}_q^B | \rho_q^j | \Psi_0 \rangle / \langle \Psi_0 | \Psi_0 \rangle^{1/2}$ , and  $\langle \bar{\Psi}_q^L | \bar{\Psi}_q^B \rangle$ . The indirect Monte Carlo orthogonalization-diagonalization process is therefore

obtained as algebraic combination of a set of basic expectation values which can be computed directly by Monte Carlo integration using a standard reweighting technique which we show in the following. The reweighting technique is needed because the Metropolis algorithm we use to generate the particle (real and shadow variables) configurations in the simulation box is able to reproduce only a strictly positive distribution probability. This is the case for the extended ground-state configuration probability:

$$\begin{aligned} P(R, S, S') &= \frac{F(R, S') F(R, S)}{\langle \Psi_0 | \Psi_0 \rangle} \\ &= \frac{F(R, S') F(R, S)}{\int dR dS dS' F(R, S') F(R, S)} \end{aligned} \quad (\text{A1})$$

[note that  $P(R, S, S')$  is not equivalent to  $|\Psi_0|^2 / \langle \Psi_0 | \Psi_0 \rangle$ ]. The average of any function  $f(R, S, S')$  can be computed in this way:

$$\begin{aligned} \langle f \rangle_{RSS'} &= \int dR dS dS' P(R, S, S') f(R, S, S') \\ &= \frac{1}{M} \sum_{\{R, S, S'\}} f(R, S, S'), \end{aligned} \quad (\text{A2})$$

where  $\{R, S, S'\}$  is the set of the configurations generated by the Metropolis algorithm.

Now consider for example the quantity  $\langle \Psi_q^C | \Psi_q^D \rangle$  which can be computed in this way:

$$\begin{aligned} \langle \bar{\Psi}_q^L | \bar{\Psi}_q^B \rangle &= \frac{\langle \Psi_q^L | \Psi_q^B \rangle}{\sqrt{\langle \Psi_q^L | \Psi_q^L \rangle} \sqrt{\langle \Psi_q^B | \Psi_q^B \rangle}} \\ &= \frac{\int dR dS dS' F(R, S') F(R, S) \bar{\delta}'_{-q} \bar{\sigma}_{-q}}{\sqrt{\int dR dS dS' F(R, S') F(R, S) \bar{\delta}'_{-q} \bar{\delta}_{-q}} \sqrt{\int dR dS dS' F(R, S') F(R, S) \bar{\sigma}'_{-q} \bar{\sigma}_{-q}}} \\ &= \frac{\int dR dS dS' P(R, S, S') \bar{\delta}'_{-q} \bar{\sigma}_{-q}}{\sqrt{\int dR dS dS' P(R, S, S') \bar{\delta}'_{-q} \bar{\delta}_{-q}} \sqrt{\int dR dS dS' P(R, S, S') \bar{\sigma}'_{-q} \bar{\sigma}_{-q}}} = \frac{\langle \bar{\delta}'_{-q} \bar{\sigma}_{-q} \rangle_{RSS'}}{\sqrt{\langle \bar{\delta}'_{-q} \bar{\delta}_{-q} \rangle_{RSS'}} \sqrt{\langle \bar{\sigma}'_{-q} \bar{\sigma}_{-q} \rangle_{RSS'}}}. \end{aligned} \quad (\text{A3})$$

The prime over the density fluctuations  $\bar{\sigma}'_q$  or  $\bar{\delta}'_q$  means that those are functions of the shadow variables  $\{S'\}$ . In a similar way quantities like  $\langle \bar{\Psi}_q^L | \hat{O} | \bar{\Psi}_q^L \rangle$  can be computed as

$$\langle \bar{\Psi}_q^L | \hat{O} | \bar{\Psi}_q^L \rangle = \frac{\left\langle \frac{\hat{O} F}{F} \bar{\delta}'_{-q} \bar{\delta}_{-q} \right\rangle_{RSS'}}{\langle \bar{\delta}'_{-q} \bar{\delta}_{-q} \rangle_{RSS'}}. \quad (\text{A4})$$

where  $F$  stands for  $F(R, S)$  or, for better statistics,  $F = \frac{1}{2}[F(R, S) + F(R, S')]$ . In a similar way the matrix elements which enter in the expression for the intensity of the excitation peaks in the dynamical structure factor can be written as



$$\begin{aligned}
\frac{\langle \bar{\Psi}_q^L | \rho_q^j | \Psi_0 \rangle}{\sqrt{\langle \Psi_0 | \Psi_0 \rangle}} &= \frac{\langle \Psi_q^L | \rho_q^j | \Psi_0 \rangle}{\sqrt{\langle \Psi_q^L | \Psi_q^L \rangle} \sqrt{\langle \Psi_0 | \Psi_0 \rangle}} \\
&= \frac{\int dR dS dS' F(R, S') F(R, S) \bar{\delta}_{-q}^j \rho_q^j}{\sqrt{\int dR dS dS' F(R, S') F(R, S) \bar{\delta}_{-q}^j \bar{\delta}_{-q}^j} \sqrt{\int dR dS dS' F(R, S') F(R, S)}} \\
&= \frac{\int dR dS dS' P(R, S, S') \bar{\delta}_{-q}^j \rho_q^j}{\sqrt{\int dR dS dS' P(R, S, S') \bar{\delta}_{-q}^j \bar{\delta}_{-q}^j}} = \frac{\langle \bar{\delta}_{-q}^j \rho_q^j \rangle_{RSS'}}{\sqrt{\langle \bar{\delta}_{-q}^j \bar{\delta}_{-q}^j \rangle_{RSS'}}} \quad (A5)
\end{aligned}$$

and

$$\frac{\langle \bar{\Psi}_q^B | \rho_q^j | \Psi_0 \rangle}{\sqrt{\langle \Psi_0 | \Psi_0 \rangle}} = \frac{\langle \bar{\sigma}_{-q}^j \rho_q^j \rangle_{RSS'}}{\sqrt{\langle \bar{\sigma}_{-q}^j \bar{\sigma}_{-q}^j \rangle_{RSS'}}}. \quad (A6)$$

With this reweighting technique any function in the extended configuration space  $\{R, S, S'\}$  is averaged with the extended configurational distribution probability of the ground state.

The orthogonalization-diagonalization process is, however, very delicate because it exploits a reweighting technique to obtain the diagonalization of the Hamiltonian directly from Monte Carlo integration. It is, in fact, well known that a lot of statistics are needed to reach the convergence of this type of algorithm: at each density about  $10^8$  Monte Carlo steps have been used to obtain these results. A calculation with this computational cost is only possible on a parallel supercomputer: we have used a CRAY-T3E with 128 processing elements to run in parallel statistically independent random walks, obtaining a linear speedup.

- 
- <sup>1</sup>L. D. Landau and I. Pomeranchuk, Dokl. Akad. Nauk SSSR **59**, 669 (1948).  
<sup>2</sup>A. Fabrocini, S. Fantoni, S. Rosati, and A. Polls, Phys. Rev. B **33**, 6057 (1986).  
<sup>3</sup>A. Fabrocini and A. Polls, Phys. Rev. B **58**, 5209 (1998).  
<sup>4</sup>E. Krotscheck, J. Paaso, M. Saarela, K. Schörkhuber, and R. Zillich, Phys. Rev. B **58**, 12 282 (1998).  
<sup>5</sup>B. Fak, K. Guckelsberger, M. Korfer, R. Scherm, and A. J. Dianoux, Phys. Rev. B **41**, 8732 (1990).  
<sup>6</sup>S. A. Vitiello, K. Runge, and M. H. Kalos, Phys. Rev. Lett. **60**, 1970 (1988); S. A. Vitiello, K. Runge, G. V. Chester, and M. H. Kalos, Phys. Rev. B **42**, 228 (1990).  
<sup>7</sup>D. E. Galli, E. Cecchetti, and L. Reatto, Phys. Rev. Lett. **77**, 5401 (1996).  
<sup>8</sup>D. E. Galli and L. Reatto, in *Condensed Matter Theories* (Nova Science, Commack, NY, 1997), Vol. 12, p. 95.  
<sup>9</sup>D. E. Galli, G. L. Masserini, S. A. Vitiello, and L. Reatto, Czech. J. Phys. **46**, 295 (1996).  
<sup>10</sup>S. Moroni, D. E. Galli, S. Fantoni, and L. Reatto, Phys. Rev. B **58**, 909 (1998).  
<sup>11</sup>C. Ebner and D. O. Edwards, Phys. Rep. **2**, 77 (1970).  
<sup>12</sup>W. Wu, S. A. Vitiello, L. Reatto, and M. H. Kalos, Phys. Rev. Lett. **67**, 1446 (1991).  
<sup>13</sup>R. P. Feynman, Phys. Rev. **94**, 262 (1954).  
<sup>14</sup>L. Reatto, S. A. Vitiello, and G. L. Masserini, J. Low Temp. Phys. **93**, 879 (1993).  
<sup>15</sup>D. E. Galli, L. Reatto, and S. A. Vitiello, J. Low Temp. Phys. **101**, 755 (1995).  
<sup>16</sup>R. A. Aziz, F. R. W. McCourt, and C. C. K. Wong, Mol. Phys. **61**, 1487 (1987).  
<sup>17</sup>S. Yorozu, H. Fukuyama, and H. Ishimoto, Phys. Rev. B **48**, 9660 (1993).  
<sup>18</sup>R. Simons and R. M. Mueller, Czech. J. Phys. **46**, 201 (1996).  
<sup>19</sup>E. Krotscheck, M. Saarela, K. Schörkhuber, and R. Zillich, Phys. Rev. Lett. **80**, 4709 (1998).  
<sup>20</sup>E. Krotscheck and M. Saarela, Phys. Rep. **232**, 1 (1993).  
<sup>21</sup>V. F. Sears, in *Neutron Scattering*, Vol. 23A of Methods of Experimental Physics, edited by K. Skold and D.L. Price (Academic, New York, 1986), p. 521.  
<sup>22</sup>J. Boronat, F. Dalfovo, F. Mazzanti, and A. Polls, Phys. Rev. B **48**, 7409 (1993).  
<sup>23</sup>Even if we have about 1% of concentration of <sup>3</sup>He we do not have Fermi statistic effects because we have just one independent fermion.